Investigation of SSR in Practical DFIG-Based Wind Farms Connected to a Series-Compensated Power System

Liang Wang, Xiaorong Xie, *Senior Member, IEEE*, Qirong Jiang, *Member, IEEE*, Hui Liu, Yu Li, and Huakun Liu

***Abstract*—Subsynchronous resonance (SSR) was observed in wind farms located in North China. These wind farms prevailingly consist of doubly-fed induction generators (DFIGs) and are connected to series-compensated transmission lines. The observed resonant frequency is about 6 ∼ 8 Hz, which is much lower than that of the reported SSR occurred in Texas. The frequency varies during the occurrence and this phenomenon is observed for the first time. The output power is usually within a certain range, when SSR occurs. Based on the practical system, an equivalent simulation system has been established, in which wind farms are modeled as many identical low rating DFIGs. Then, the SSR event is reproduced by simulations. Analysis results indicate that SSR happens even when the equivalent transmission system compensation level seen from wind farms is only 6.67%. Eigenvalue analysis shows that this phenomenon is an electrical resonance, and could be affected considerably by wind speed, number and control of DFIGs. The number of in-service DFIGs has a nonlinear impact on the damping of SSR. An equivalent electric circuit is deduced to intuitively explain why SSR happens and how the above factors affect it. Considering its features, this phenomenon is recognized as DFIG control participated induction generator effect.**

***Index Terms*—Doubly-fed induction generator, fixed series capacitor, induction generator effect, subsynchronous control interaction, subsynchronous resonance.**

I. Introduction

As a source of clean energy, wind power has been exploited vigorously in many countries. In China, large-scale development and utilization of wind energy has become an integral part of national energy strategy [1]. In recent years, many wind power bases have been established in north and west of China. However, the main load center of China is located in the east and south of China so that the utilization of wind energy highly relies on high-rating and long-distance transmission.

Manuscript received June 17, 2014; revised August 21, 2014 and September 23, 2014; accepted October 21, 2014. Date of publication November 06, 2014; date of current version July 17, 2015. This work was supported in part by the National Natural Science Foundation of China under Grant 51322701 and in part by the 863 Project of China under Grant 2012AA050215. Paper no. TPWRS-00818-2014. (*Corresponding author: X. Xie.*)

L. Wang is with the School of Automation, Beijing Institute of Technology, Beijing 100081, China (e-mail: s.wl@live.cn).

X. Xie, Q. Jiang, and Huakun Liu are with the State Key Laboratory of Power System, Department of Electrical Engineering, Tsinghua University, Beijing 100084, China (e-mail: xiexr@tsinghua.edu.cn; qrjiang @tsinghua.edu.cn; goodliuhuakun@163.com).

Hui Liu and Y. Li are with the North China Electric Power Research Institute, Beijing 100045, China.

Color versions of one or more of the figures in this paper are available online at http://ieeexplore.ieee.org.

Digital Object Identifier 10.1109/TPWRS.2014.2365197

Since fixed series capacitors (FSCs) can significantly improve transmission capacity and stability margin of power system [2] with relatively lower cost than thyristor controlled series capacitors (TCSCs), it is widely applied in large-scale transmission of remote electric power. However, FSCs may induce subsynchronous resonance (SSR). In October 2009, a wind farm in Texas of USA suffered from an accident caused by FSCs, resulting in a number of wind turbine generators (WTGs) tripped and damage of many crowbar circuits of doubly-fed induction generators (DFIGs) [3]. This phenomenon is called subsynchronous control interaction (SSCI) in [3]. It is named as subsynchronous interaction (SSI) in [4] and recognized as SSR in [5]. After this accident, a lot of research has been conducted on this SSR phenomenon between DFIGs and series-compensated power systems. Reference [4] points out that, in series compensated systems, DFIGs are more vulnerable to SSR compared to fixed speed WTGs and WTGs connected by back-to-back converters. The SSR of DFIG based wind farms has been analyzed by eigenvalue analysis, impedance model, and time domain simulations [5]–[8]. It is found that the higher compensation level and the lower wind speed, the less damping of the resonance. In several literature, the critical total line compensation levels were relatively high, more than 50% [5]–[7], when SSR appeared. The total line compensation level is defined as the ratio of impedance of FSC to the impedance of all the transmission lines and transformers between the wind farm and the infinite bus. However, such high compensation levels are generally unacceptable in practice. Noticeably, the previous studies paid close attention on the influence of series compensation level, wind speed, rotor side converter (RSC) control parameters on the frequency and damping of SSR. In these literature, all WTGs in a widely distributed wind farm are simplified into one large-rating generator. It has not been analyzed whether the number of grid-connected WTGs could affect the SSR. Also, the analysis in the aforementioned literature has not been benchmarked with actual SSR events and the mechanism of SSR caused by DFIG has not been explained in an intuitively understandable way. This paper makes efforts on the above points based on actual SSR events happened in North China.

On December 25, 2012, SSR was observed in certain wind farms located in the north of China and caused many WTGs tripped. Several similar events happened in the subsequent weeks. The resonant frequency is about 6 ∼ 8 Hz in these events, which is much lower than 20 Hz, the resonant frequency of the SSR event that happened in Texas [3], and those reported in [5]–[7]. Another interesting characteristic is that the SSR frequency varies during the event and is not the same in

different events, which has not been reported or explained by previous literature. The wind farms are more vulnerable to SSR when the output power is within a certain range. The number of WTGs in service is considered in the system model and a nonlinear impact on SSR damping is observed for the first time.

In Section II, one of these actual SSR events will be presented in details. Then, the practical wind farm and series compensated transmission network are modeled in Section III. The SSR event is reproduced by time-domain simulations in Section IV. In Section V, the equivalent system is analyzed using eigenvalue analysis to get the influence on SSR from wind speed, number of grid-connected WTGs, and converter control parameters. Further, an electric circuit based analysis is presented in Section VI to intuitively illustrate the mechanism of this type of SSR. The conclusion is drawn in Section VII.

II. SSR Event of the Wind Farms

A. Wind Farms and Series-Compensated System

The wind farms, where SSR events have been recorded, and their transmission networks are shown in Fig. 1. These wind farms are located in Hebei Province, North China. Twenty-three wind farms over a vast area are collected by 220-kV lines and connected to a centralized step-up station. Then, the electric power is stepped up to 500 kV and transmitted via 500-kV series-compensated lines to the North China Grid. By the end of 2012, the total installed capacity of WTGs in this area has exceeded 3000 MW. Most of these WTGs are 1.5-MW DFIGs and very few are permanent magnet synchronous generators and self-excited induction generators.

B. SSR Event

On about 8:47 am, December 25, 2012, many WTGs in this area were suddenly tripped, meanwhile the step-up transformer vibrated abnormally and made loud noise. According to the data from fault recorder at the step-up station, large magnitude subsynchronous currents at about 7 Hz were observed, as shown in Fig. 2. Considering the series compensation in 500-kV lines, this accident was deemed as an unstable SSR.

Fig. 2 shows that the voltage is distorted slightly, but the amplitude of subsynchronous currents is nearly the same as the amplitude of fundamental frequency currents.

Discrete Fourier transformation (DFT) is applied on the recorded data to obtain more information. The RMS values at both fundamental and subsynchronous frequencies of the currents at the 220-kV side of the step-up transformer are obtained and shown in Fig. 3, from which, the development of the SSR event can be clearly recognized. Fig. 3 shows that the fault recorder has recorded data for about 500 s during this event. But the duration of SSR must be longer than 500 s, because the fault recorder could be triggered only when the fault current is large enough. According to Fig. 3(a), the SSR event could be divided into 4 stages:

1) At the beginning of the SSR event, the subsynchronous currents diverged quickly, while the fundamental currents remained nearly unchanged.
2) When the amplitude of subsynchronous currents grew to a very large value, the protection of generators was triggered to trip WTGs. After many WTGs were tripped, both fundamental and subsynchronous currents decreased immediately.

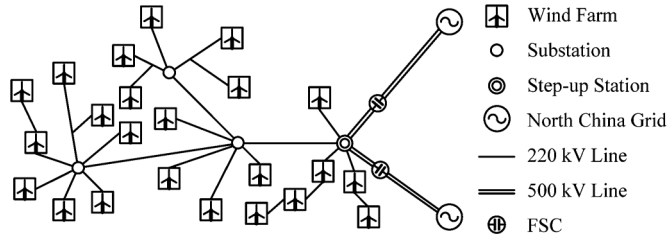

Fig. 1. Wind farms and the series-compensated system.

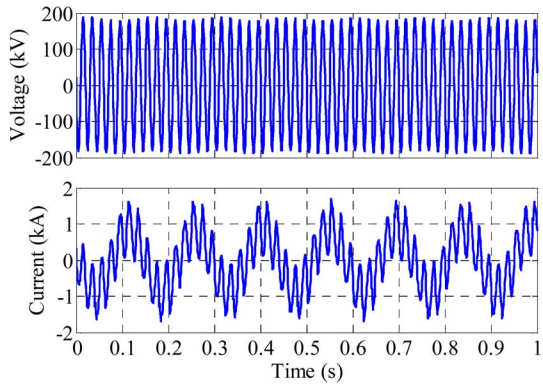

Fig. 2. Voltage and current of a-phase at the 220-kV side of step-up station during the SSR event.

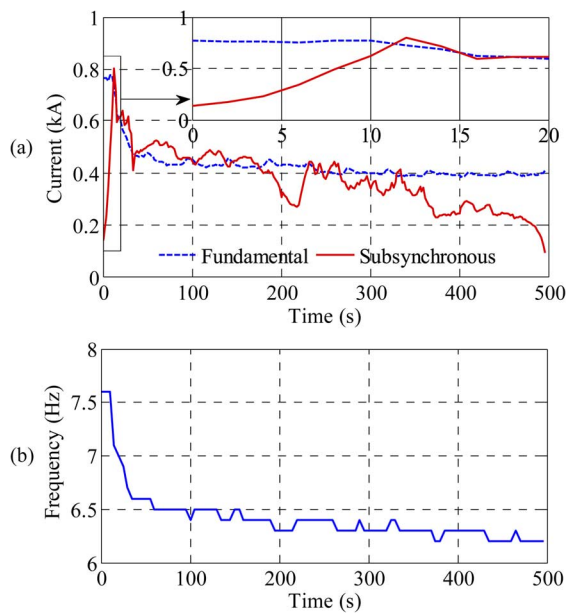

Fig. 3. DFT results of currents at the 220-kV side of step-up station: (a) RMS value of currents at different frequencies, (b) Frequency of the subsynchronous currents.

3) Then, the amplitude of subsynchronous currents fluctuated with time, but decreased very slowly in general. SSR seemed to be near a critical stable state. The amplitude of fundamental currents fluctuated with the random variation of wind velocity and decreased when more WTGs were tripped.
4) Finally, the subsynchronous currents damp out quickly and the SSR event ended.

Fig. 3(b) shows that the frequency of subsynchronous currents decreased from 7.6 Hz to 6.2 Hz during the SSR event. It

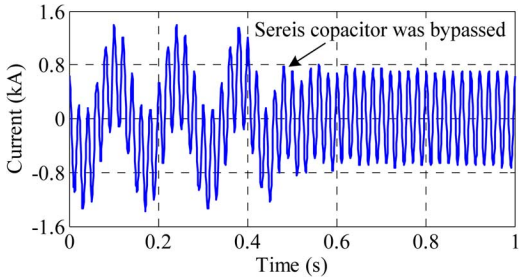

Fig. 4. Subsynchronous currents disappear immediately after the series capacitors are bypassed.

could be observed that there is a strong correlation in the variation of amplitude and frequency of subsynchronous currents.

In another SSR event of this area captured on February 1, 2013, the series capacitors of one compensated 500-kV circuit were manually bypassed when sufficiently large subsynchronous currents were detected. Consequently, the subsynchronous currents disappeared immediately, as shown in Fig. 4. Hence, bypassing FSCs, when SSR is detected, is adopted as a temporary SSR solution at present.

Besides the aforementioned events, several other SSR incidents were also observed. The basic characteristics of these events are summarized as follows:

1) The frequency of subsynchronous resonance is usually within the range of $6 \sim 8$ Hz. The frequency varies during each SSR event and the variation process differs from one to another event.
2) The SSR phenomena have direct relationship with the FSCs and are affected by the operating status of the wind farms, such as the number of WTGs in service and the wind speed.
3) SSR usually happens when the output power of wind farms is decreasing and the power is within the range of $100 \sim 300$ MW ($0.26 \sim 0.79$ kA at the 220-kV side) in most SSR cases. In other words, the system damping to SSR will be enhanced when the output power is out of this range.

III. Modeling of Wind Farms and Transmission System

The practical system as shown in Fig. 1 is too complex to analyze. A comparatively simplified equivalent system is necessary for time-domain simulations and some other analysis. Though the parameters of the WTGs and the length of feeder lines could affect the critical stability point of SSR, it has acceptable precision if all of the WTGs are modeled as one aggregated generator [9]. To check the impact of the WTG number on SSR, the wind farms are modeled by a large number of identical low-rating WTGs, which are connected to one collection bus. This system is equivalent to the one with an aggregated generator when the number of WTGs is given.

Supposing: 1) all the generators in this area are DFIGs of the same type; 2) the operating states of the same type devices are the same when they are in service, the complex system in Fig. 1 could be simplified to an equivalent system shown in Fig. 5, where n is the number of WTGs in service.

In these wind farms, Sinovel SL1500 WTGs rated at 1.5 MW are widely installed. For simplicity, we assume all online generators in this area are DFIGs of this type. Their parameters, as listed in Table I, and operating status are the same. A two-mass drive train model is adopted to represent the shaft of WTGs [9],

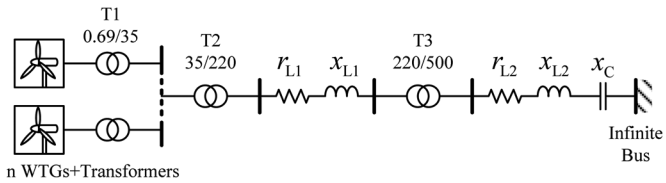

Fig. 5. Equivalent system of the wind farms and series-compensated system.

TABLE I
Parameters of DFIG and T1 (Base Capacity = 1.5 MVA)

Item	Value (p.u.)	Item	Value (p.u.)
Stator resistance r_s	0.022	T1 Resistance r_{T1}	0.015
Stator reactance x_s	0.28	T1 reactance x_{T1}	0.06
Rotor resistance r_r	0.027	Mutual reactance x_m	12.9
Rotor reactance x_r	0.31		

TABLE II
Parameters of Transmission Network (Base Capacity = 1500 MVA)

Item	Value (p.u.)	Item	Value (p.u.)
r_{L1}	0.01	x_C	0.024
x_{L1}	0.10	x_{T2}	0.06
r_{L2}	0.005	x_{T3}	0.14
x_{L2}	0.06		

[10]. The time constant of wind turbine and generator rotor are 2.5 s and 0.5 s separately. Elastic coefficient of the shaft is 0.35 p.u./rad [10]. Mechanical damping of the shaft system is neglected. Hence, if all of the turbines provide electricity to the grid, there is $n = 2000$. In other words, n should be an integer number smaller than 2000 if not all turbines are in service.

The 220-kV radial grid is represented with equivalent line inductance x_{L1} and resistance r_{L1}. x_{L1} is calculated by the short circuit capacity supplied by the wind farms to the 220-kV side bus of step-up station. For the 500-kV series-compensated grid, equivalent inductance x_{L2} is obtained using the impedance of the 500-kV system without series compensation seeing from the step-up station. Capacitance x_C is calculated using the difference at 7 Hz of x_{L2} and the impedance considering series compensation. r_{L1} and r_{L2} are calculated using typical ratio of resistance to inductance in 220-kV and 500-kV transmission lines. The parameters of the equivalent transmission network are listed in Table II.

According to the equivalent system, a medium compensation rate ($0.024/0.06 = 40\%$) is adopted for the 500-kV lines. However, the total line compensation level of the whole system viewing from the collection bus of wind farms, as defined in (1), is very low, only 6.67%:

$$k = \frac{x_C}{x_{T2} + x_{T3} + x_{L1} + x_{L2}}. \tag{1}$$

As illustrated in Fig. 6, maximum power point tracking (MPPT) of DFIG is realized by looking up table of wind speed and rotor speed [5]. Table III shows the relationship of wind speed, rotating speed and output power of the wind turbine. It is clear that the wind turbine keeps minimum rotating speed when the wind speed is lower than 5 m/s and keeps maximum speed when the wind speed is higher than 8 m/s. Under other conditions, the rotating speed is directly proportional to wind speed. The control algorithm of RSC and GSC are shown in Fig. 7. The RSC controls the rotor speed according to wind

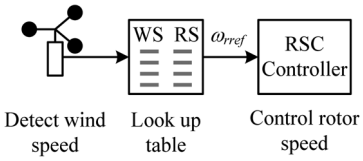

Fig. 6. MPPT algorithm.

TABLE III
WIND SPEED, ROTATING SPEED, AND THE CORRESPONDING OUTPUT POWER

WS	RS	OP	WS	RS	OP
3	0.667	0.003	8	1.200	0.500
4	0.667	0.048	9	1.200	0.710
5	0.667	0.110	10	1.200	0.931
6	0.844	0.200	10.5	1.200	1.000
7	1.022	0.326	25	1.200	1.000

Note: WS: Wind speed in m/s; RS: Rotating Speed in p.u.; OP: Output Power in p.u.

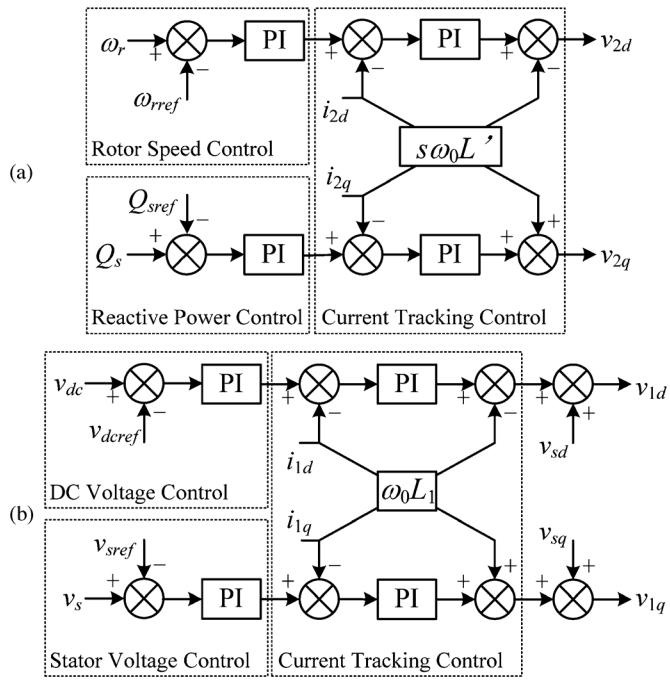

Fig. 7. Control block diagram of DFIG. (a) Control block diagram of RSC. (b) Control block diagram of GSC.

speed and keeps the power factor of the stator output to be unity. Usually, dynamic reactive power compensation (SVC or STATCOM) are adopted to keep the bus voltage of the wind farm in an acceptable range. Here, this task is integrated into the function of the GSC to simplify the equivalent system and its analysis. Hence, GSC maintains DC bus voltage and generator terminal voltage to be the rated value. Table IV lists the nomenclature of symbols in Fig. 7.

IV. REPRODUCTION OF THE SSR EVENT IN SIMULATION

The equivalent system is implemented in PSCAD/EMTDC. At the beginning of the simulation, the wind speed is 6 m/s. In consideration of the unequal distribution of wind over the vast area, a small number of WTGs are out of service and 1700 WTGs are operated normally. Then, the wind speed decreases to 5.1 m/s and SSR phenomenon arises. Once the subsynchronous currents reach certain amplitude, some WTGs are tripped from the power system. The system turns into a critical stable operating state. After that, the changes of velocity of wind and number of WTGs affect directly the stability of SSR. The simulation results are presented in Fig. 8.

TABLE IV
SYMBOLS IN CONTROL BLOCK DIAGRAMS OF RSC AND GSC

Symbols	Meaning
ω_r	Electrical angular speed of rotor
ω_0	Rated angular speed of stator
Q_s	Output reactive power of stator
s	Slip
L'	Cross coupling inductance
i_{2d}	Direct-axis component of RSC output current
i_{2q}	Quadrature-axis component of RSC output current
v_{2d}	Reference of d-axis component of RSC output voltage
v_{2q}	Reference of q-axis component of RSC output voltage
v_s	RMS value of generator terminal voltage
v_{dc}	DC voltage
i_{1d}	d-axis component of GSC output current
i_{1q}	q-axis component of GSC output current
v_{sd}	d-axis component of terminal voltage
v_{sq}	q-axis component of terminal voltage
v_{1d}	Reference of d-axis component of GSC output voltage
v_{1q}	Reference of q-axis component of GSC output voltage
L_1	Connection reactance of GSC
X_{ref}	Reference value of X

Fig. 8(a) shows that the voltage is distorted slightly, smaller than $\pm 1\%$, during the SSR incident. Fig. 8(b) indicates that the frequency of SSR varies in the range of 6.2 $\sim$ 7.5 Hz and changes with the wind speed and number of WTGs. As shown in Fig. 8(c), the change of current amplitude gives a clear description of the SSR process. 1) Before t_1, the system operates steadily with 1700 WTGs in service and the wind speed is 6 m/s. 2) After t_1, as the wind speed decrease to 5.1 m/s, SSR starts immediately and the amplitude of subsynchronous currents increases gradually at the frequency of 7.5 Hz. 3) At t_2, the subsynchronous currents are as large as the fundamental currents and run over the fault current level of DFIGs; hence, many WTGs drop off; 1060 WTGs are remaining in operation after t_2 and the resonant frequency decreases to 6.4 Hz at the same time. 4) At t_3, a stronger blast of wind comes; the amplitude of subsynchronous currents damps quickly. 5) At t_4, a weaker blast of wind comes; the amplitude of subsynchronous currents diverges fast. 6) After t_5, the WTGs in service decreases to 1000 and SSR tends to attenuate. 7) At t_6, another stronger blast of wind comes and the system damping is increased. 8) After t_6, the subsynchronous currents damp continuously; meanwhile, the frequency decreases to 6.2 Hz. Simulation results indicate that wind farms which prevailingly consist of DFIGs face the risk of SSR even the total compensation level is only 6.67%.

Compared to the practical SSR event, the simulation could also be divided into stages I $\sim$ IV: SSR starts and the subsynchronous currents rise gradually in stage I; in stage II, many WTGs drop out due to large subsynchronous currents; during stage III, the system operates near a critical stable point and the subsynchronous currents varies with the fluctuation of wind speed; the SSR damps out in stage IV. Comparing Fig. 8 with

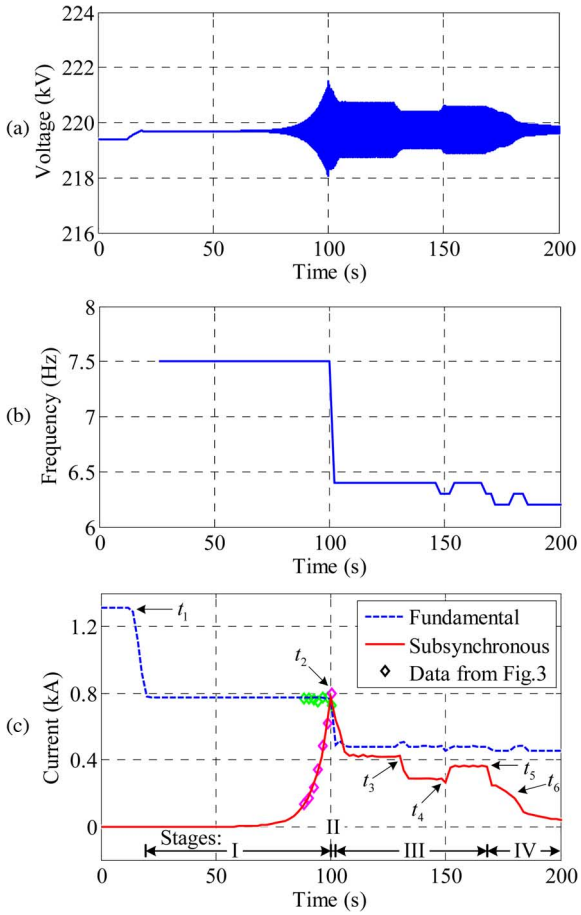

Fig. 8. Simulation results of equivalent system. (a) 220-kV side voltage of T2. (b) Frequency of subsynchronous currents. (c) DFT results of 220-kV side current.

Fig. 3, we could find that time-domain simulation of the equivalent system gives an acceptable reproduction of the practical SSR event, especially during the fast-divergence period. Thus, the equivalent system is of reliable precision.

The natural frequency of the WTG shaft used in the equivalent system is about 1.8 Hz. It could be observed that the frequency of SSR is far from the natural frequency of WTG shaft and its complementary frequency. Hence, this SSR phenomenon is not the traditional torsional interaction.

In another simulation, the subsynchronous currents will immediately disappear if the series capacitor is bypassed when SSR happens. This coincides with the practical phenomenon presented in Fig. 4.

V. Eigenvalue Analysis of the Equivalent System

Eigenvalue analysis based on linearized system model is conducted to check the impacts of several key factors on SSR.

A. Participation Factors

Table V lists the participation factors of key variables in SSR mode when the wind speed is 8 m/s and 1500 WTGs are in service. The participation factors show that key electrical variables have strong impacts on SSR while the variables of shaft contribute nearly nothing to SSR. It indicates that SSR is an electrical resonance phenomenon and the torsional oscillation is not involved.

TABLE V
Participation Factors of Key Variables in SSR Mode

Variables	Factors
Position angle of wind turbine	0.000
Position angle of generator rotor	0.000
Speed of wind turbine	0.000
Speed of generator rotor	0.000
d-axis component of stator input current	0.974
q-axis component of stator input current	1.000
d-axis component of rotor input current	0.9329
q-axis component of rotor input current	0.9633
d-axis component of transmission line current	0.0389
q-axis component of transmission line current	0.0396
d-axis component of series capacitor voltage	0.0787
q-axis component of series capacitor voltage	0.0786

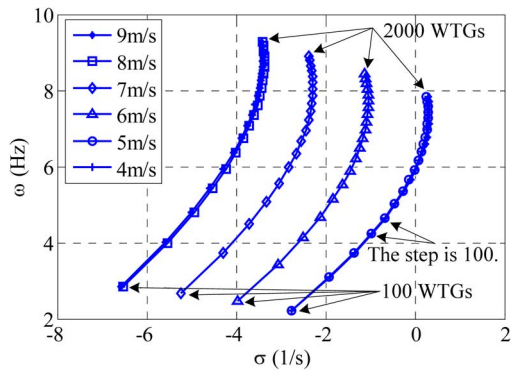

Fig. 9. Impacts on SSR from velocity of wind and number of WTGs.

B. Impacts From Wind Speed and Number of WTGs

The variations of eigenvalues are presented in Fig. 9 when wind speed and the number of WTGs vary, where σ and ω are respectively the real part and imagery part of the eigenvalues related to SSR.

Considering the relationship between wind speed and rotor speed in Table III, Fig. 9 displays that the system damping has a positive correlation with the rotor speed. The higher the rotor speed, the larger the system damping. But the number of WTGs performs a nonlinear influence on SSR damping. Under the condition of a given wind speed, there is certain number of WTGs which will induce worst damping effect. Under this condition, the damping will increase whether the number increases or decreases.

Fig. 9 also shows that SSR usually happens when the wind is weak and certain number of WTGs are in service, which means that the output power is in a certain range, and the frequency of SSR is in the range of 6 $\sim$ 8 Hz. These characteristics coincide with practical SSR events.

C. Impacts From Line Parameters

Figs. 10 and 11 present the influence on SSR from series capacitor and total resistance of the transmission line when the wind speed is 8 m/s and the number of WTGs is 1500.

Fig. 10 indicates that the system damping decreases and the frequency increases with the rise of series compensation. As shown in Fig. 11, the damping increases with the rise of total line resistance, but the frequency changes slightly.

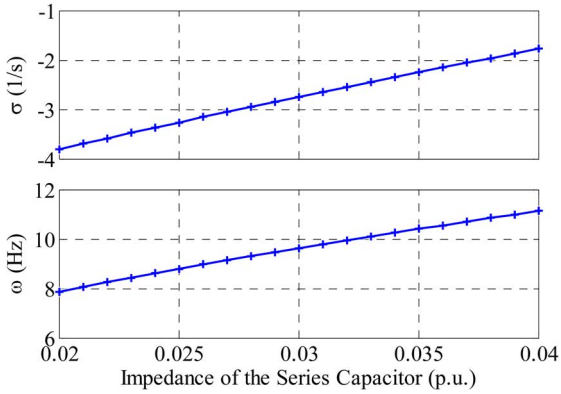

Fig. 10. Impact on SSR from the variation of series capacitor.

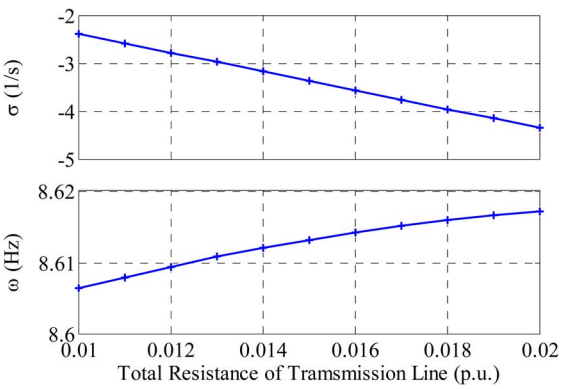

Fig. 11. Impact on SSR from the variation of total transmission line resistance.

D. Impacts From DFIG Control Parameters

The impacts on SSR from the control parameters of RSC and GSC are evaluated when these parameters change between 0.1 $\sim$ 10 times of those used in the above analysis under the condition that velocity of wind is 8 m/s and 1500 WTGs are in service. Analysis results indicate that proportional gains of RSC current tracking control, stator reactive power control, DC voltage control, and stator voltage control perform strong impacts on SSR. The impacts of the above four parameters are presented in Fig. 12. Impacts from other control parameters are smaller than from the above parameters.

Fig. 12 indicates that control parameters of RSC have the strongest impacts on SSR, especially the proportional gain of RSC current tracking control. The system damping decreases dramatically with the increase of proportional gain of RSC current tracking control.

Taking all the results of eigenvalue analysis into account, it could be found that this kind of SSR phenomenon of DFIG based wind farms, which are connected to series-compensated power system, is a kind of electrical resonance and the control loops play important roles.

VI. Equivalent Circuit Based Analysis

An equivalent circuit of wind farms is deduced in this section to provide a more intuitive explanation of the mechanism of SSR phenomenon in DFIG based wind farms. The circuit is very similar to that for traditional IGE analysis except the participation of DFIG control. Hence, it is recommended to describe this type of SSR as DFIG control participated IGE.

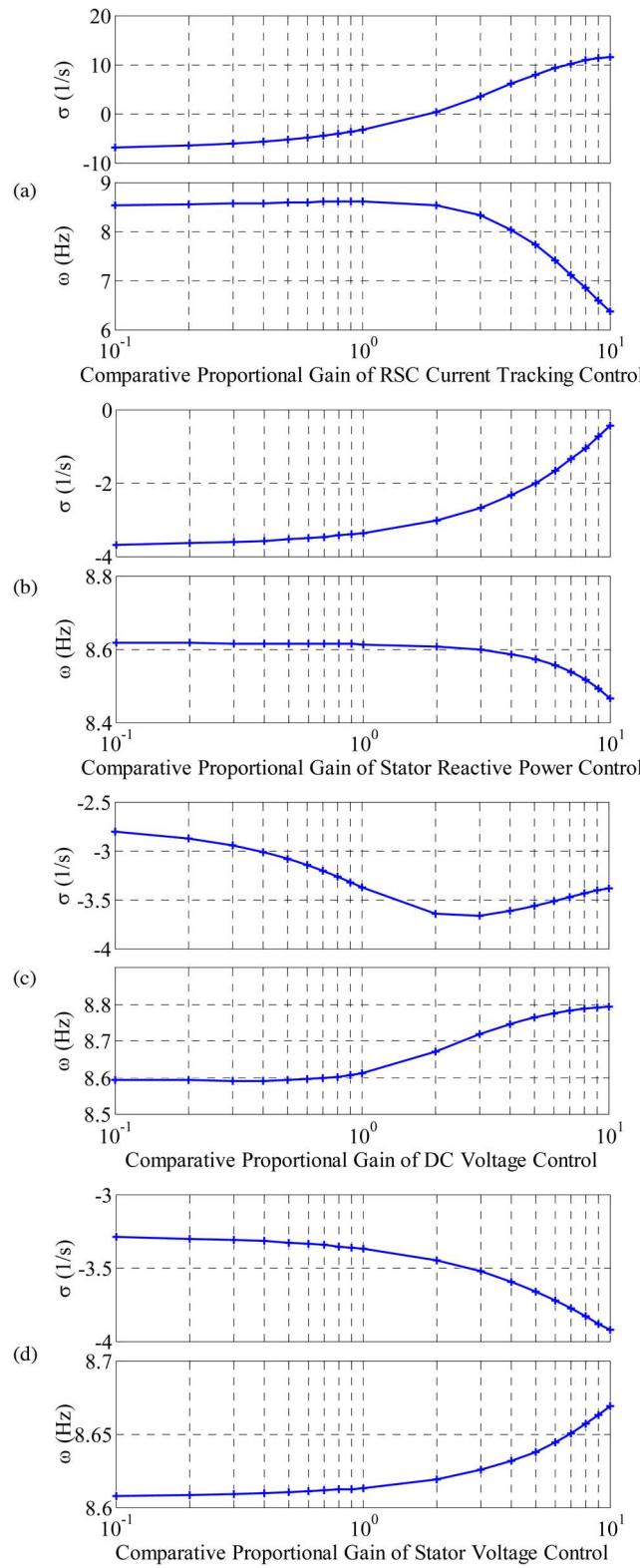

Fig. 12. Influences on SSR from variation of control parameters.

A. Equivalent Circuit

The simple circuit shown in Fig. 13 has been widely adopted to analyze the traditional IGE phenomenon of steam turbine generators [11], where $s = (\omega - \omega_r)/\omega$ is the slip of rotor to

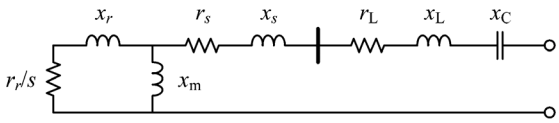

Fig. 13. Equivalent circuit adopted in IGE analysis.

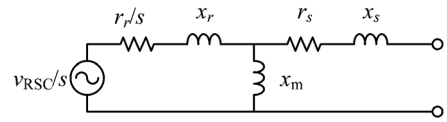

Fig. 14. Equivalent circuit of DFIG.

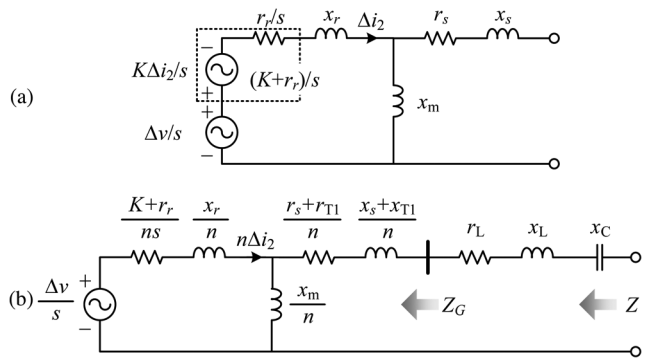

Fig. 15. Equivalent circuit. (a) Equivalent circuit of DFIG for disturbances. (b) Equivalent circuit for the whole system.

stator currents at the frequency of ω. It gives a well explanation of IGE mechanism and illustrates the impacts on SSR from many factors, such as slip s, rotor resistance r_r, line resistance $r_{\rm L}$, series capacitance $x_{\rm C}$, and so on.

According to the analysis above, the RSC has much stronger impacts on SSR compared to GSC. Hence, GSC could be neglected in this circuit-based analysis. If only the RSC is taken into consideration, the DFIG could be represented by Fig. 14 [10], where $v_{\rm RSC}$ is the converted output voltage of RSC.

Supposing the current references of RSC are constant while there is a disturbance $\Delta\mathbf{i}_{2dq} = [\Delta i_{2d}\ \Delta i_{2q}]^{\rm T}$ in rotor currents, the resulted disturbance in output voltage of RSC will be

$$\Delta\mathbf{v}_{2dq} = -K\Delta\mathbf{i}_{2dq} + \Delta\mathbf{v}_{dq} \tag{2}$$

where $\Delta\mathbf{v}_{2dq} = [\Delta v_{2d}\ \Delta v_{2q}]^{\rm T}$, K is the proportional gain of RSC current tracking control, $\Delta\mathbf{v}_{dq} = [\Delta v_d\ \Delta v_q]^{\rm T}$ is a disturbance caused by some other factors of the controller, such as decoupling control and integration control of RSC controller. Considering (2), the DFIG model could be represented by Fig. 15(a) when only the mentioned disturbances are taken into consideration. The function of $-K\Delta\mathbf{i}_{2dq}$ is the same as a resistance of K. Noticeably, we suppose n DFIGs are synchronized to the system. Thus, the whole equivalent system can be described by an electric circuit shown in Fig. 15(b), where

$$\begin{cases} r_L = r_{L1} + r_{L2} \\ x_L = x_{L1} + x_{L2} + x_{T2} + x_{T3}. \end{cases} \tag{3}$$

As discussed above, K exerts most powerful impact on SSR in the control of DFIG. Hence, the $\Delta v/s$ could be neglected in the primary analysis. Thus, there is

$$\begin{aligned} Z_G(\omega) &\approx \frac{1}{n}\left[r_s + r_{T1} + j\omega(x_s + x_{T1}) \right. \\ &\qquad \left. + j\omega x_m // \left(\frac{K + r_r}{s} + j\omega x_r\right)\right] \\ &= R_G(\omega) + jX_G(\omega) \end{aligned} \tag{4}$$

$$\begin{aligned} Z(\omega) &= r_L + j\left(\omega x_L - \frac{x_C}{\omega}\right) + Z_G(\omega) \\ &= R(\omega) + jX(\omega). \end{aligned} \tag{5}$$

B. Equivalent Circuit Based Analysis

At a subsynchronous frequency ω_n, if there is $R(\omega_n) < 0$ and $X(\omega_n) \approx 0$, a diverging electrical resonance, or SSR, will happen at ω_n.

At subsynchronous frequencies, there is $s < 0$. Hence, the DFIG could provide negative damping for SSR. The higher the rotor speed, the larger the $|s|$. Hence, the absolute value of $(K + r_r)/ns$ is smaller when the rotor operates at higher speed. This means that the DFIG will generate less energy at the subsynchronous frequency. In other words, DFIG will provide less negative damping for the SSR. Hence, the SSR damping increases with the rise of rotor speed.

Obviously, the number of WTGs, n, could change the equivalent inductance $X_G(\omega)$. A larger n will result in a smaller X_G, which means that resonant frequency of the whole system will increase when more WTGs are in service. This phenomenon coincides with the data of fault recorder and its DFT results shown in Fig. 3. This impact could be much stronger when the number of WTGs is smaller as shown in Fig. 9, because X_G is proportional to $1/n$.

While $\omega x_{\rm m}$ is large enough, it could be neglected from the equivalent circuit. Under this condition, larger n will result in smaller $|(K+r_r)/ns|$. Therefore, the system damping increases when n becomes larger. When n is smaller below a certain level, the resonant frequency is too low to keep $\omega x_{\rm m}$ large enough. While a small $\omega x_{\rm m}$ is taken into consideration, the final equivalent resistance $|R_G(\omega)|$ will become smaller. Thus, the system damping is enhanced. These observations well explain the nonlinear impact on SSR damping from DFIG.

Obviously, the system damping will increase with the rise of line resistance $r_{\rm L}$. While the series compensation level becomes higher, the resonant frequency will increase, which will result in a smaller $|s|$, and then less damping.

The proportional gain K of RSC controller increases the equivalent resistance of DFIG rotor. Hence, a larger K results in much more negative resistance and smaller system damping. It should be pointed out that some disturbances in other control loops of RSC, which can be represented by Δv, could also change the negative damping of SSR.

These features obtained from the equivalent circuit match the results of eigenvalue analysis very well. Hence, the equivalent circuit is acceptable to explain this type of SSR phenomenon.

Comparing Fig. 13 with Fig. 15, it could be found that the mechanism of SSR happened in DFIG based wind farms is similar to the traditional IGE. A different but key point is that the

RSC of DFIG changes the equivalent impedance of the rotor and makes the system more vulnerable to SSR. Eigenvalue analysis reveals that GSC control also exerts influence on system damping. Hence, it is reasonable to recognize this phenomenon as DFIG control participated IGE, which could give a well explanation of the mechanism and characteristics of this type of SSR.

VII. Conclusions

In this paper, an actual SSR event occurred in wind farms located in North China is presented and its entire process is reproduced by time-domain simulation with an equivalent system model. Eigenvalue-based analyses have been further conducted to investigate the impacts on the SSR characteristics from the parameters of the grid and the DFIGs. An equivalent circuit, which could provide reasonable mechanism explanation of SSR, is also induced. The main conclusions are drawn as follows:

1) Wind farms based on DFIGs face potential risk of SSR when they are connected to a series-compensated power system, even if the total compensation level is very low (for instance, 6.67% in our reported event).
2) Resonant frequency varies during a single SSR event, which is mainly caused by the variation of the number of the DFIGs. This frequency variation presents a new challenge for the analysis of and identifying a solution to this type of SSR associated with widely spread wind farms.
3) This DFIG-associated SSR is a type of control participated electrical resonance, without the involvement of torsional interaction. In addition to the various influential factors of the system side and environment, the control parameters of both RSC and GSC have great impact on its characteristics. Hence, it can be described as DFIG control participated IGE.
4) The control of DFIG, especially the control of RSC, changes the equivalent impedance of DFIG and thus greatly affects the damping and frequency of the potential resonance, which makes DFIGs more vulnerable to SSR.
5) The number of in-service DFIGs has an obvious but nonlinear impact on the system damping.

References

[1] W. Zhongying, *R&D of Chinese Strategic new Industries: Wind Energy*. Beijing, China: China Machine Press, 2013.

[2] A. A. Fouad and K. T. Khu, "Subsynchronous resonance zones in the IEEE "bench mark" power system," *IEEE Trans. Power App. Syst.*, vol. PAS-97, pp. 754–762, May 1978.

[3] J. Adams, C. Carter, and S.-H. Huang, "ERCOT experience with subsynchronous control interaction and proposed remediation," in *Proc. Transmission and Distribution Conf. Expo. 2012*, pp. 1–5.

[4] ABB Inc., ERCOT CREZ Reactive Power Compensation Study, Dec. 2010.

[5] L. Fan, R. Kavasseri, Z. L. Miao, and C. Zhu, "Modeling of DFIG-based wind farms for SSR analysis," *IEEE Trans. Power Del.*, vol. 25, no. 4, pp. 2073–2082, Oct. 2010.

[6] L. Fan, C. Zhu, Z. Miao, and M. Hu, "Modal analysis of a DFIG-Based wind farm interfaced with a series compensated network," *IEEE Trans. Energy Convers.*, vol. 26, no. 4, pp. 1010–1020, Dec. 2011.

[7] Z. Miao, "Impedance-model-based SSR analysis for type 3 wind generator and series-compensated network," *IEEE Trans. Energy Convers.*, vol. 27, no. 4, pp. 984–991, Dec. 2012.

[8] G. D. Irwin, A. K. Jindal, and A. L. Issacs, "Sub-synchronous control interaction between type 3 wind turbines and series compensated AC transmission systems," in *Proc. 2011 IEEE PES General Meeting*, pp. 1–6.

[9] R. K. Varma and A. Moharana, "SSR in double-cage induction generator-based wind farm connected to series-compensated transmission line," *IEEE Trans. Power Syst.*, vol. 28, no. 3, pp. 2573–2583, Aug. 2013.

[10] Y. Lei, A. Mullane, G. Lightboby, and R. Yacamini, "Modeling of the wind turbine with a doubly fed induction generator for grid integration studies," *IEEE Trans. Energy Convers.*, vol. 21, no. 1, pp. 257–264, Mar. 2006.

[11] P. Kundur, *Power System Stability and Control*. New York, NY, USA: McGraw-Hill, 1994.

Liang Wang received the B.S. degree from the Department of Electrical Engineering, Shandong University, Jinan, China, in 2007, the M.S. degree from the Department of Electricity, South China University of Technology, Guangzhou, China, in 2010, and the Ph.D. degree from the Department of Electrical Engineering, Tsinghua University, Beijing, China, in 2014, all in electrical engineering.

He is now a lecturer of the School of Automation, Beijing Institute of Technology, Beijing, China. His research interests include subsynchronous resonance analysis and solutions, modeling and control of the flexible AC transmission systems (FACTS), and improving the stability and power quality of the power system using FACTS devices.

Xiaorong Xie (M'02–SM'14) received the B.Sc. degree from Shanghai Jiao Tong University, Shanghai, China, in 1996 and the Ph.D./M.Eng. degrees from Tsinghua University, Beijing, China, in 2001.

From 2001 to 2005, he was a Lecturer with the Department of Electrical Engineering, Tsinghua University. Since 2005, he has worked as an Associate Professor in the same department. His current research interests focus on subsynchronous resonance evaluation and its counter-measures, power system analysis and control based on wide-area measurements, and flexible ac transmission systems.

Qirong Jiang (M'98) received the B.S. and Ph.D. degrees in electrical engineering from Tsinghua University, Beijing, China, in 1992 and 1997, respectively.

In 1997, he joined the Department of Electrical Engineering, Tsinghua University as a Lecturer. He later became an Associate Professor in 1999. Since 2006, he has been a Professor. His research interests include power system analysis and control, modeling and control of flexible AC transmission systems, power quality analysis and mitigation, power electronic equipments, and renewable energy power conversion.

Hui Liu received the M.S. degree in electrical engineering from Shandong University, Jinan, China, in 2001 and the Ph.D. degree in electrical engineering from Tianjin University, Tianjin, China, in 2005.

He is currently working for North China Electric Power Research Institute. His interests include power system operation and security analysis.

Yu Li is currently working for North China Electric Power Research Institute. His interests include power system operation and security analysis.

Huakun Liu was born in Shandong province, China, in 1991. He received the B.S. degree from Shandong University, Jinan, China, in 2013. He is pursuing the M.S. degree at Tsinghua University, Beijing, China.

His research interests include power system stability analysis and control.